Supplement of Atmos. Chem. Phys., 21, 9931–9953, 2021
https://doi.org/10.5194/acp-21-9931-2021-supplement
© Author(s) 2021. CC BY 4.0 License.

Atmospheric Chemistry and Physics
Open Access
EGU

Supplement of

Measurement report: The influence of traffic and new particle formation on the size distribution of 1–800 nm particles in Helsinki – a street canyon and an urban background station comparison

Magdalena Okuljar et al.

Correspondence to: Magdalena Okuljar (magdalena.okuljar@helsinki.fi)

The copyright of individual parts of the supplement might differ from the article licence.

Supplement

Correction of UCPC data at the background station

During 29.05-06.04.2018 the nighttime ratio between PSM and UCPC concentrations as well as between UCPC and CPC concentrations drifted in opposite directions. At the same time, the ratio between PSM and CPC stayed constant, which indicated that concentrations measured by UCPC drifted. This drift could be caused by a change in measuring parameter, for example, an increase in the aerosol flow. To correct this error, we divided the average nighttime ratio between UCPC and CPC from period 3.05-28.05.2018 by the nighttime ratio between these instruments for period 29.05-4.06.2018. We obtained following correlation parameters: 0.97 (29.05-30.05), 0.89 (31.05-01.06), 0.87 (02.06 and 04.06), and 0.92 (03.06). The distribution of the correction is presented at Fig S1 (a). It is much smaller than the standard deviation of UCPC data for corrected period (σ= 11 515 cm^{-3}). Figure S1 (b,c) present the difference in concentration measured by UCPC and CPC (N_{3-7}) as well as PSM and UCPC (N_{1-3}) during this campaign. UCPC correction is smaller than these concentrations, but it strongly influences the sub-3 nm concentrations measured for this period. This correction was applied only to a fraction of data at the background station, and it does not influence any analysis done for overlapping data between stations.

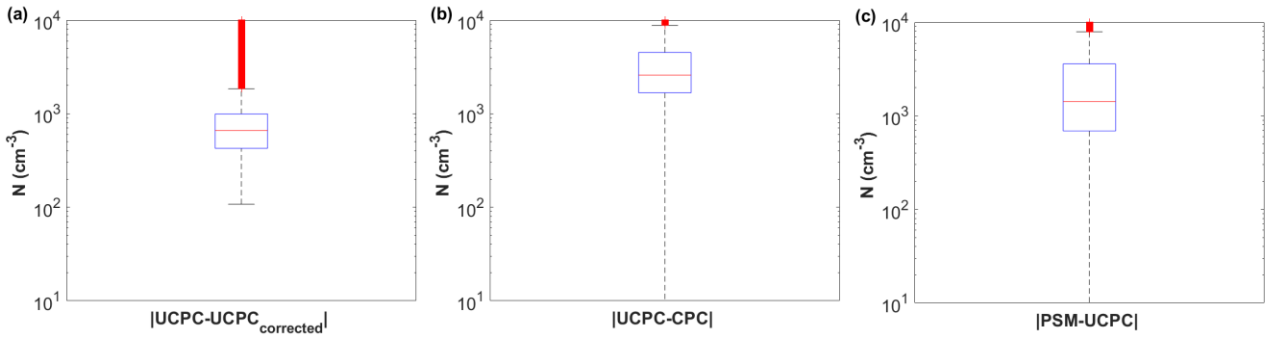

Figure S1. The distribution of the correction applied to data measured by UCPC during period 29.05-06.04.2018 (a), and the difference between concentrations measured by UCPC and CPC (b) as well as PSM and UCPC (c) during this campaign. Box plots present 25th, 50th (median), and 75th percentile values. The whiskers extend to the most extreme data points not considered outliers, and the outliers are plotted individually using the '+' symbol

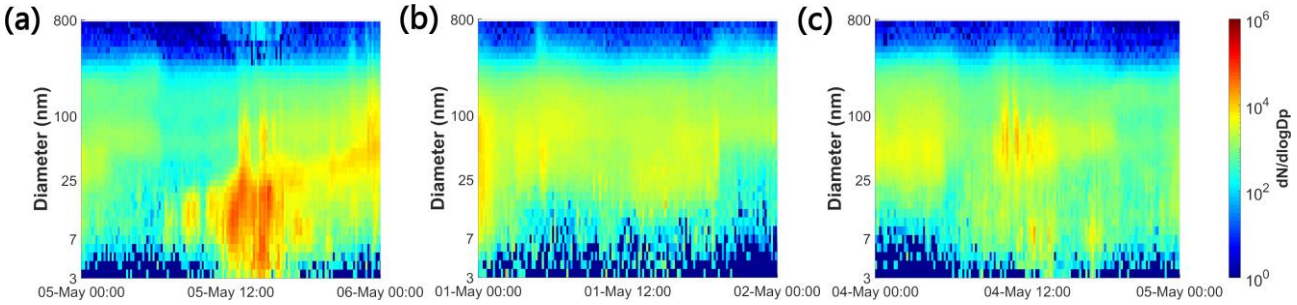

Figure S2. Example of an event (a), non-event (b), and undefined (c) class.

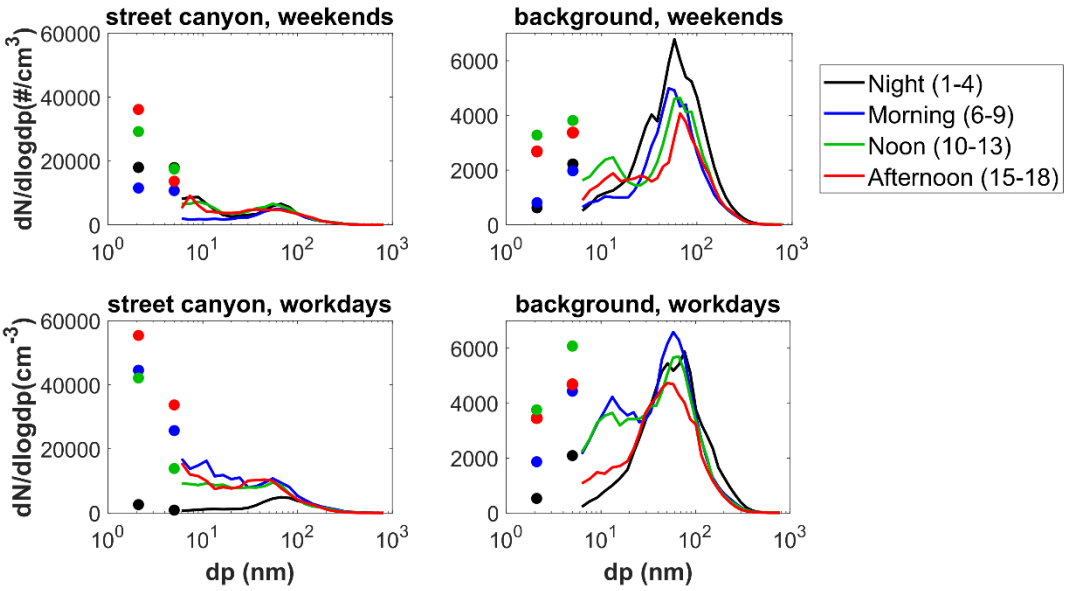

Figure S3. Median size distribution (a,c) at the street canyon and (b,d) at the background station. The colors indicate different periods of the day: night (1:00-4:00 LT, black), morning (6:00-9:00 LT, blue), noon (10:00-13:00 LT, green), and afternoon (15:00-18:00, red). The top row presents sixe distribution measured during weekends (a,b) and the bottom one during workdays (c,d). Median size distribution was determined by DMPS (particles with sizes between 6-800 nm) marked with solid lines in the figure, UCPC, and CPC (3-7 nm), and PSM and UCPC (1-3 nm) marked with dots. Each station has different limits of a y-scale.

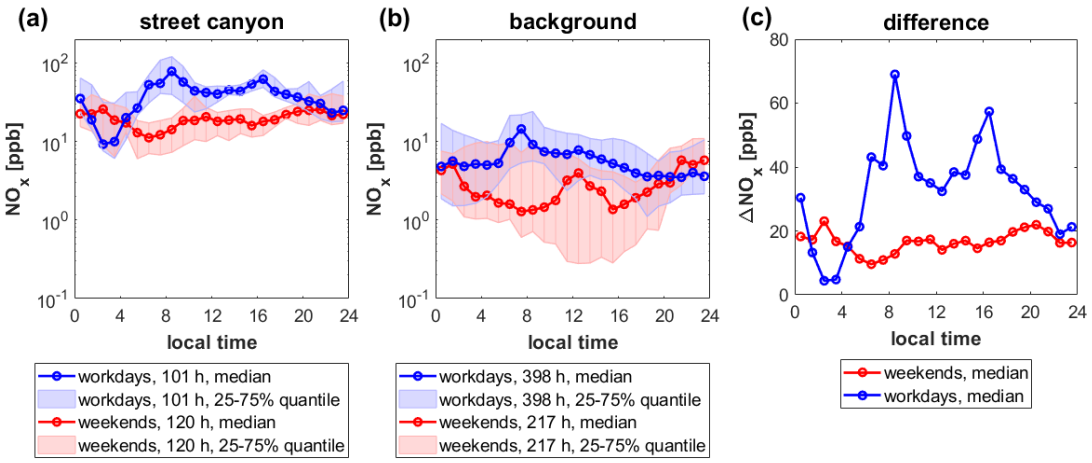

Figure S4. The diurnal variation of NOx concentration during weekends (red) and workdays (blue) (a) at the street canyon and (b) at the background station, and (c) the difference between median NOx concentration at the street canyon site and at the background station. The median diurnal variation is shown as a solid line with markers; the 25th and 75th percentile range are presented as a shaded area.

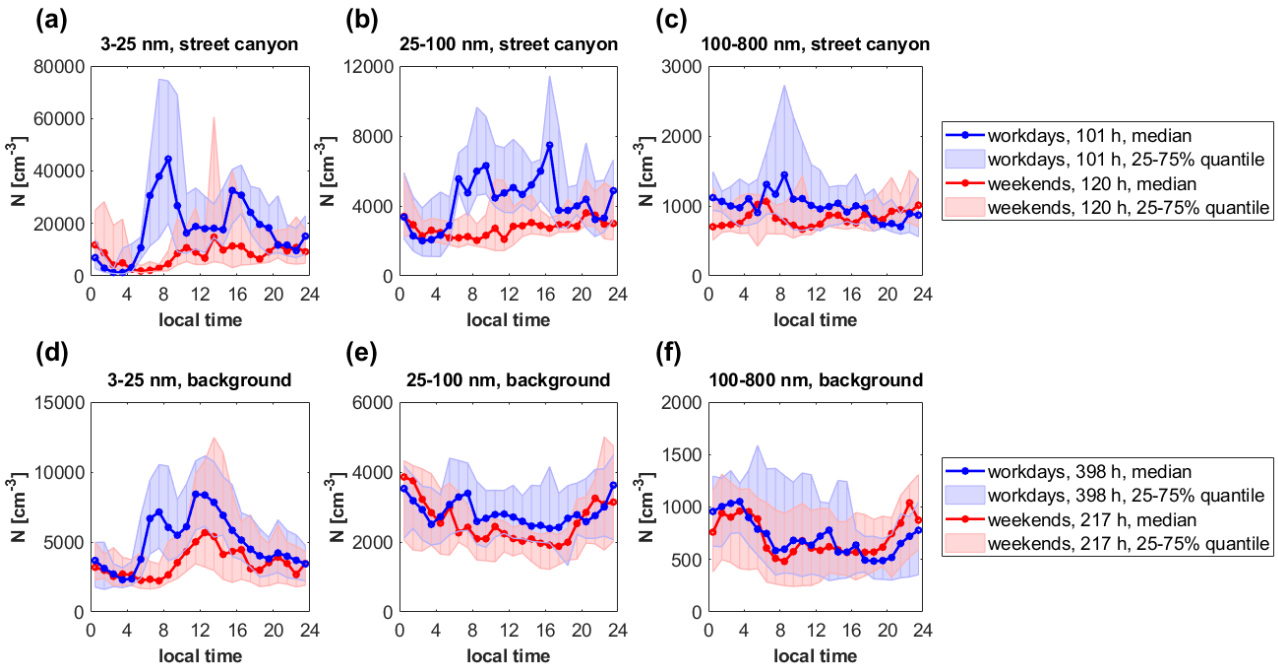

33

34 Figure S5. Diurnal variations of nucleation (3-25 nm), Aitken (25-100 nm), and accumulation (100-800 nm) modes
35 particle concentration during weekends (red) and workdays (blue) measured at the street canyon (top) and at the
36 background station (bottom). The median diurnal variation is shown as a solid line with markers; the 25th and 75th
37 percentile range are presented as a shaded area. Each subplot has different limits of a y-scale.

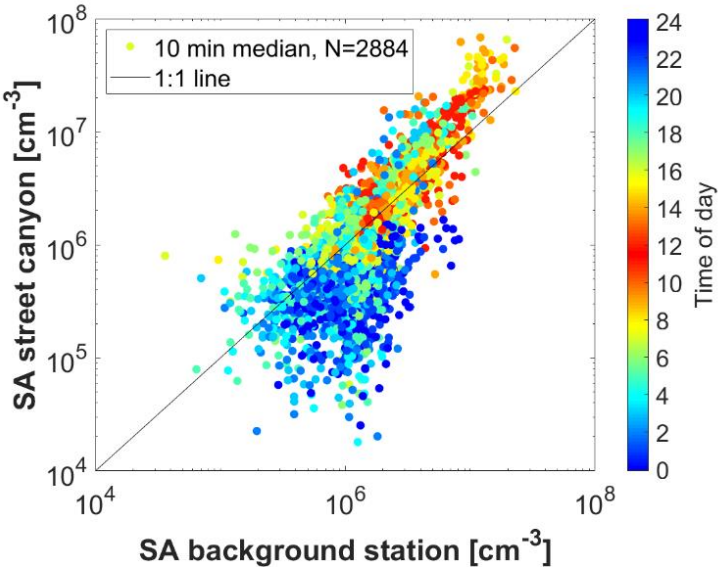

38 Figure S6. Correlation between the SA measured at the street canyon and at the background station colored by the time
39 of the day. The black line shows the 1:1 line.

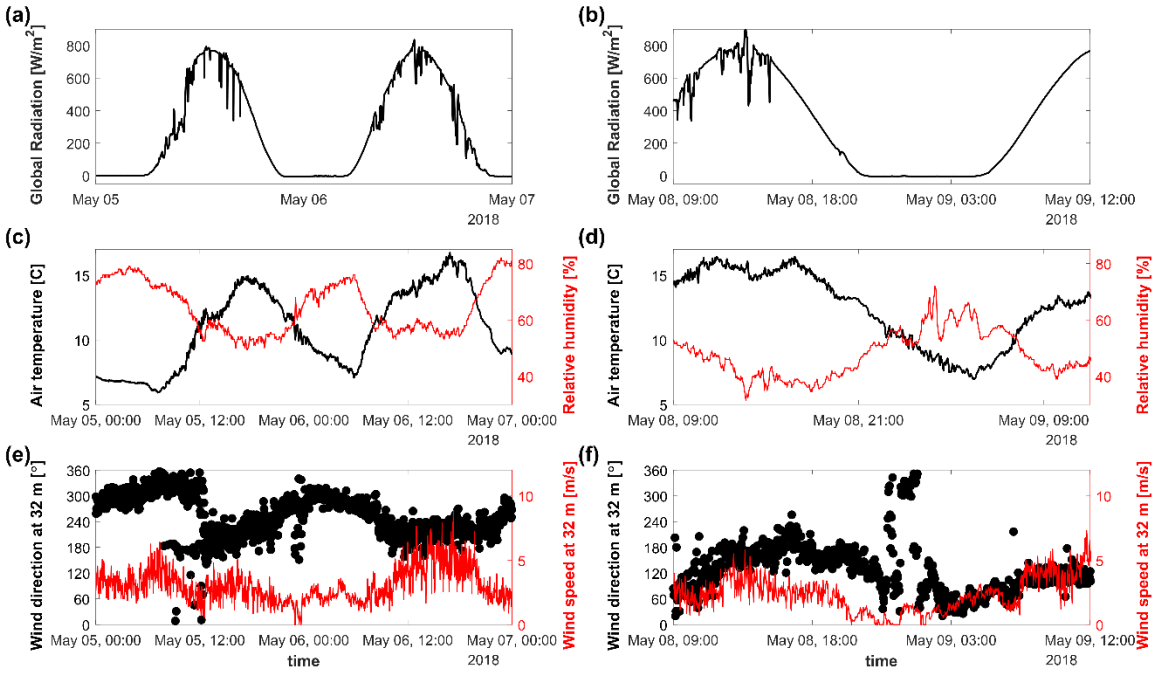

40 Figure S7. Time series of meteorological parameters (global radiation: (a) and (b), air temperature and relative humidity:
41 (c) and (d), wind direction and wind speed: (e) and (f)) measured at background station for periods 5 May 2018-7 May
42 2018 LT (left) and 8 May 2018 09:00-9 May 2018 15:00 LT (right).

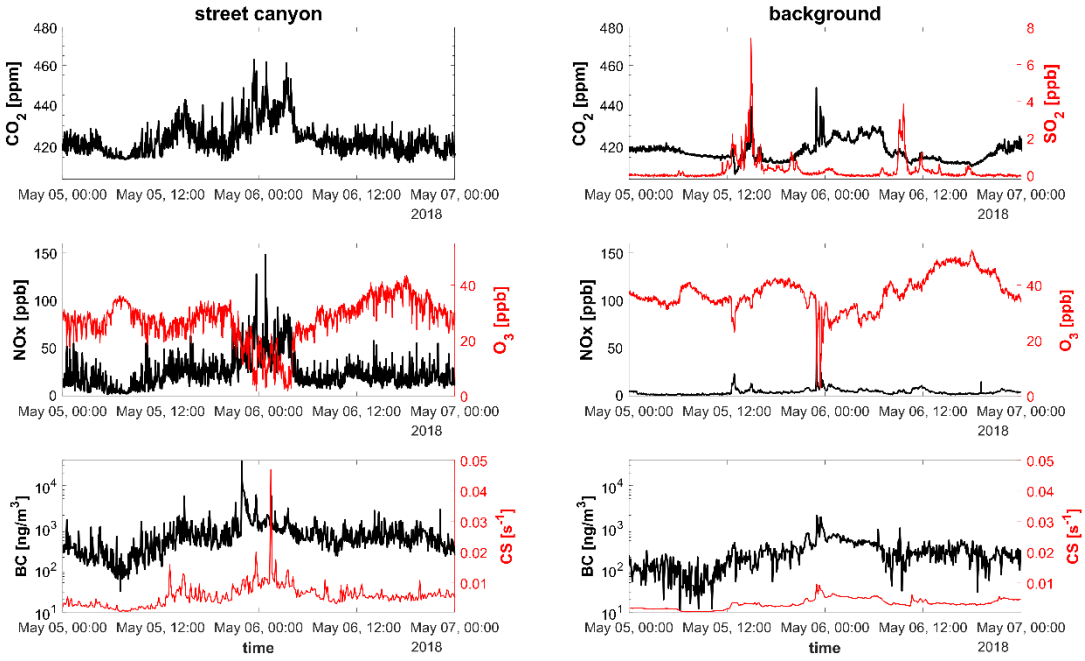

43 Figure S8. Time series of (a, b) SO_2 and CO_2 concentrations, (c, d) NO_x and O_3 concentrations, (e, f) black carbon
44 concentration (BC) and condensation sink (CS) measured at the street canyon (left) and at the background station (right)
45 for period 5 May 2018-6 May 2018 LT.

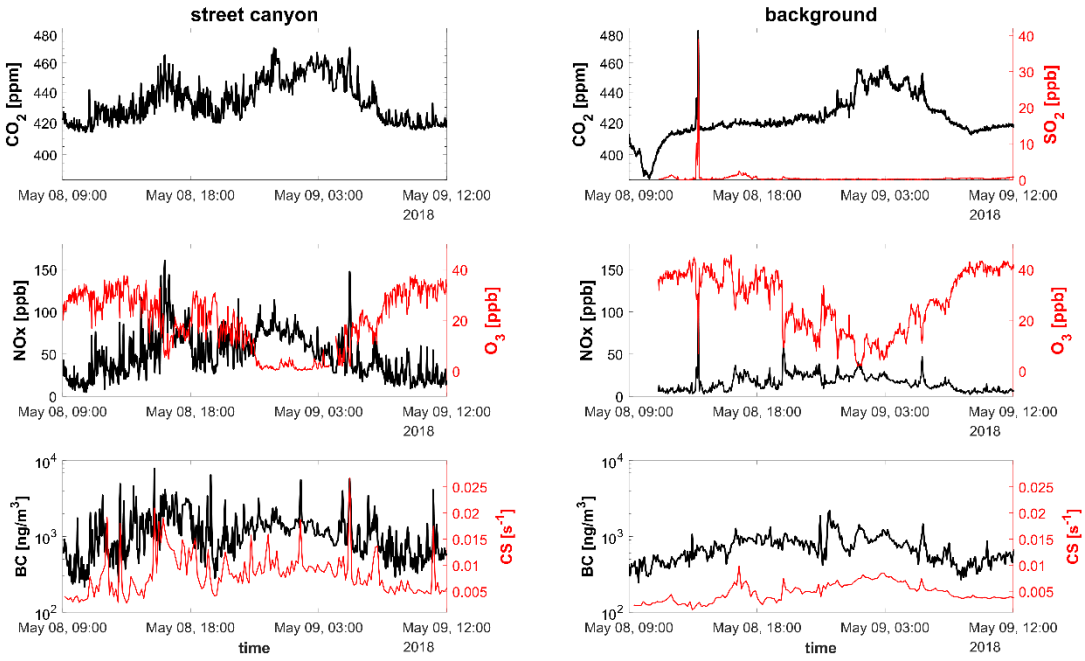

Figure S9. Time series of (a, b) SO_2 and CO_2 concentrations, (c, d) NO_x and O_3 concentrations, (e, f) black carbon concentration (BC) and CS measured at the street canyon (left) and at the background station (right) for period 8 May 2018 09:00-9 May 2018 15:00 LT.

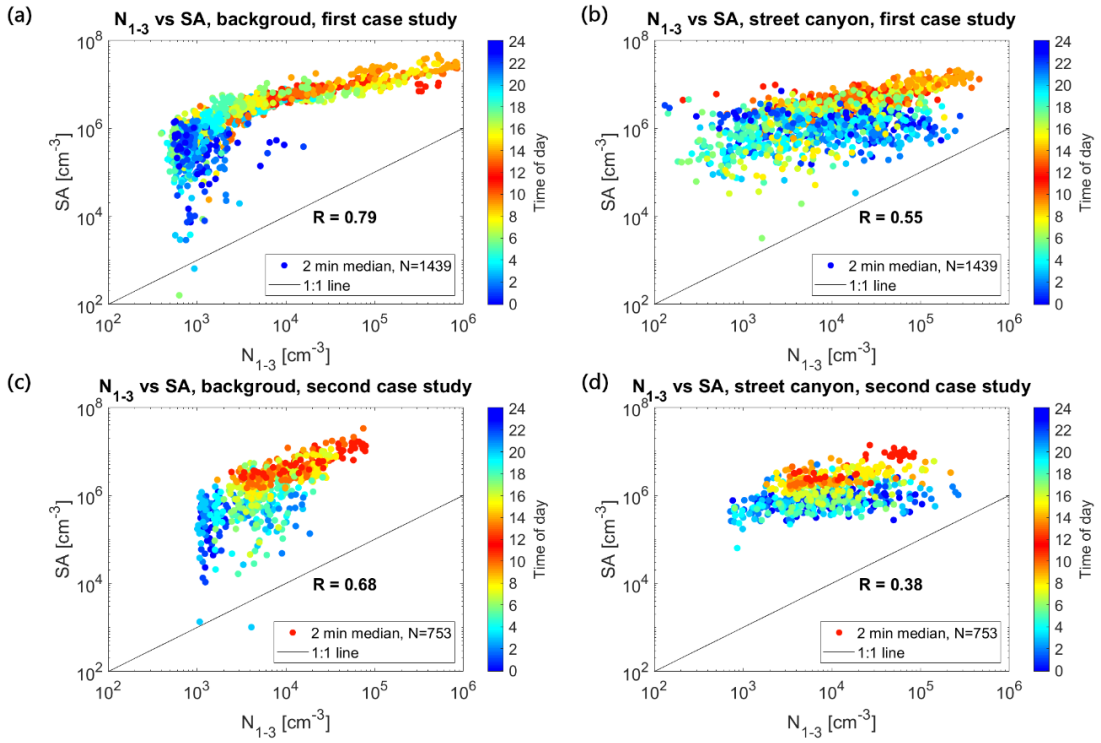

Figure S10. Correlation between the sub-3 nm particles and SA measured at the background station (a,c) and at the street canyon (b,d) for period 5 May 2018-6 May 2018 LT (a,b) and 8 May 2018 09:00-9 May 2018 15:00 LT (c,d) colored by the time of the day. The black line shows the 1:1 line.

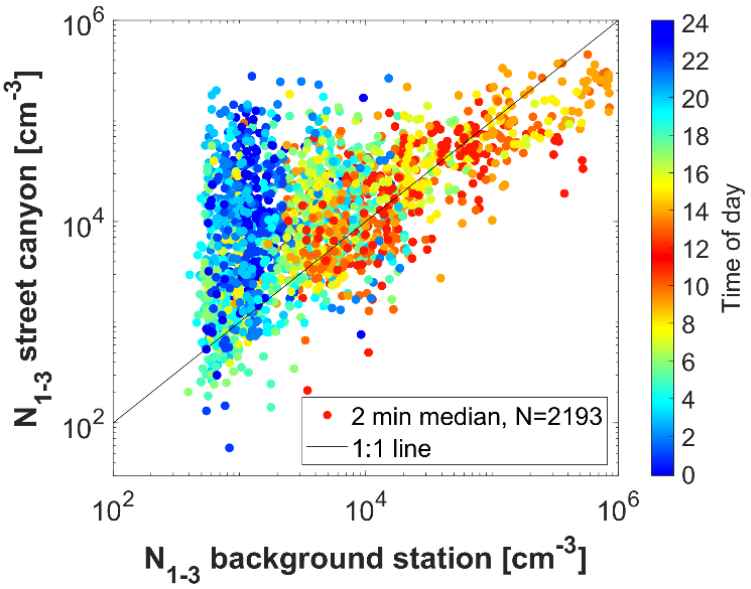

Figure S11. Correlation between the sub-3 nm particles measured at the street canyon site and at the background station colored by the time of the day for the time of both case studies. The black line shows the 1:1 line.

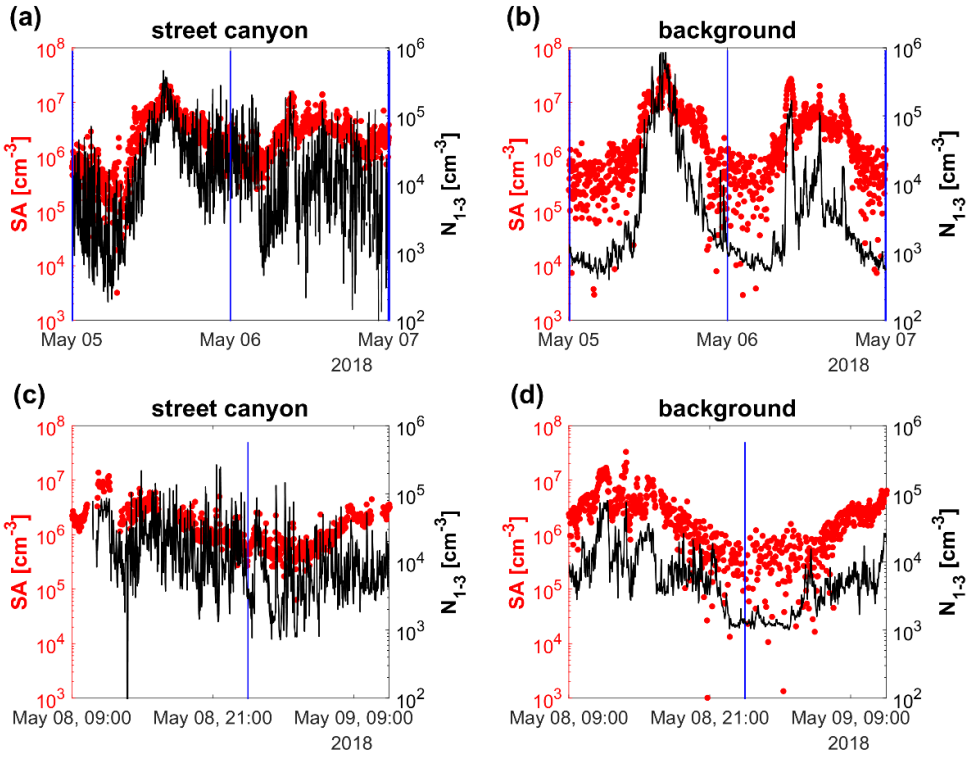

Figure S12. Time series of sub-3 nm particles (black) and SA (red) concentrations at the street canyon (a, c) and at the background station (b, d) during 5 May 2018-7 May 2018 LT (a, b) and 8 May 2018 09:00-9 May 2018 15:00 LT (c, d). Vertical blue lines indicate midnights.

Table S1. Sample size for correlation analysis between logarithmic values of $N_{1\text{-}3}$, $N_{3\text{-}7}$, $N_{7\text{-}25}$, and $N_{25\text{-}100}$ and logarithmic values of other variables during weekends and workdays at the street canyon and the background station.

Parameter		Street canyon site				Background station			
		$N_{1\text{-}3}$	$N_{3\text{-}7}$	$N_{7\text{-}25}$	$N_{25\text{-}100}$	$N_{1\text{-}3}$	$N_{3\text{-}7}$	$N_{7\text{-}25}$	$N_{25\text{-}100}$
SA [#/cm^3]	Workdays	552	2060	2488	2488	2366	2450	3455	3455
	Weekends	696	1428	3915	3915	1467	1329	1584	1584
BC [ng/m^3]	Workdays	552	2060	2488	2488	2366	2402	3402	3402
	Weekends	418	857	856	856	1467	1327	1582	1582
CS [s^{-1}]	Workdays	552	2060	2488	2488	2366	2450	3455	3455
	Weekends	418	857	856	856	1467	1329	1584	1584
NO [ppb]	Workdays	552	2060	2488	2488	1813	1802	2552	2552
	Weekends	696	1428	3915	3915	892	758	913	913
NO_x [ppb]	Workdays	552	2060	2488	2488	2218	2299	3455	3455
	Weekends	696	1428	3915	3915	1439	1301	1584	1584
O_3 [ppb]	Workdays	552	2060	2488	2488	2366	2450	3455	3455
	Weekends	696	1428	3915	3915	1467	1329	1584	1584
CO_2 [ppm]	Workdays	552	2060	2488	2488	689	715	763	763
	Weekends	696	1428	3915	3915	603	603	720	720
SO_2 ** [ppb]	Workdays	-	2060	2242	2242	2051	2182	3149	3149
	Weekends	-	1428	256	256	1266	1126	1372	1372
RH*** [%]	Workdays	552	2060	2488	2488	2366	2450	3455	3455
	Weekends	696	1428	3915	3915	1467	1329	1584	1584
T*** [°C]	Workdays	552	2060	2488	2488	2366	2450	3455	3455
	Weekends	696	1428	3915	3915	1467	1329	1584	1584
cos(WD) & sin(WD)**	Workdays	552	2060	2488	2488	2366	2450	3455	3455
	Weekends	696	1428	3915	3915	1467	1329	1584	1584

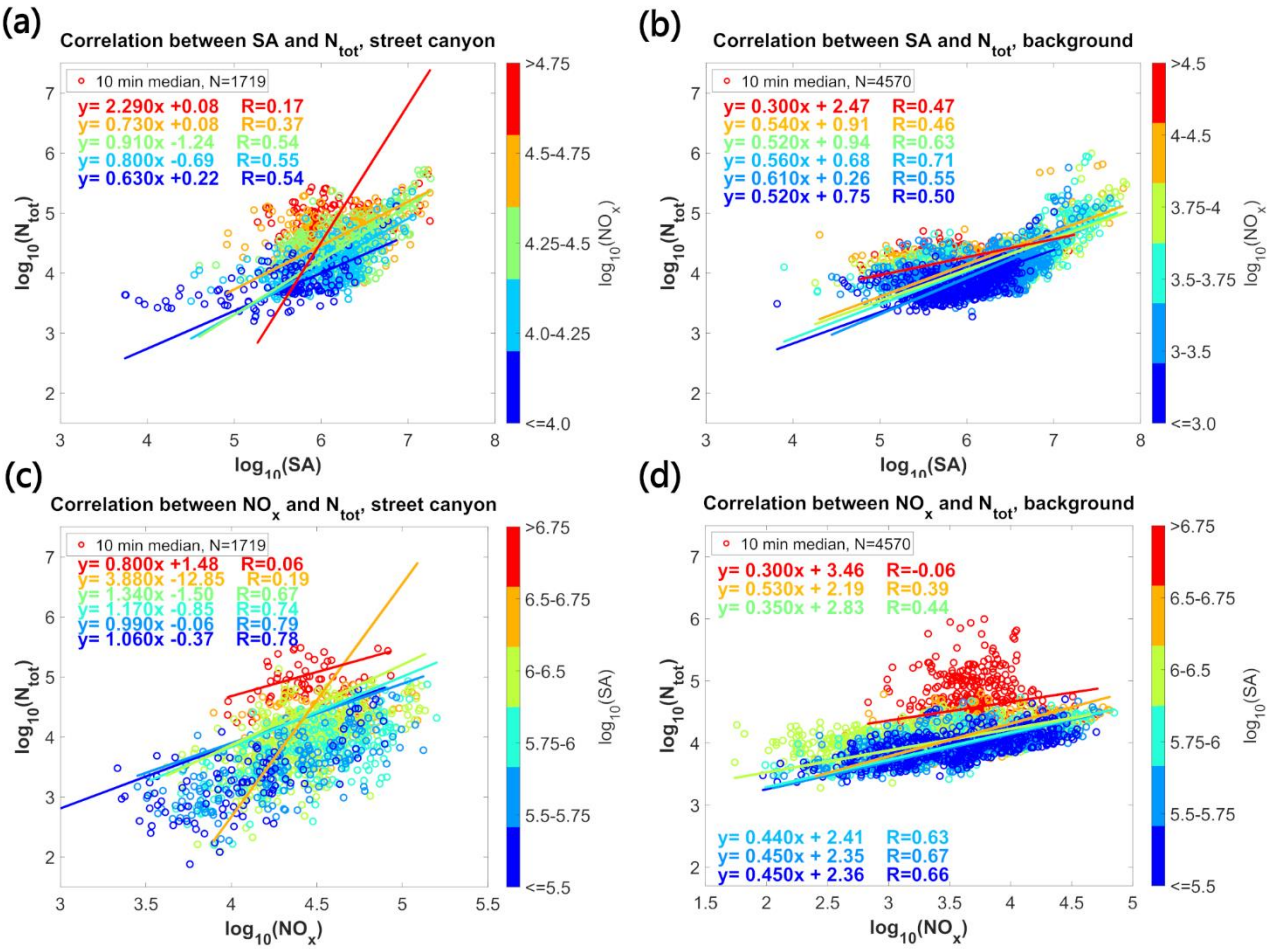

Figure S13. Correlation between the logarithm of SA and the logarithm of the total concentration of particles (N_{tot}) colored by the logarithm of NO_x (a) at the street canyon and (b) the background station, as well as the correlation between the logarithm of NO_x and the logarithm of N_{tot} particles colored by the logarithm of SA (c) at the street canyon and (d) at the background station. Lines represent bivariate fit done to data. The parameters of the fit are presented as an equation on the plot.

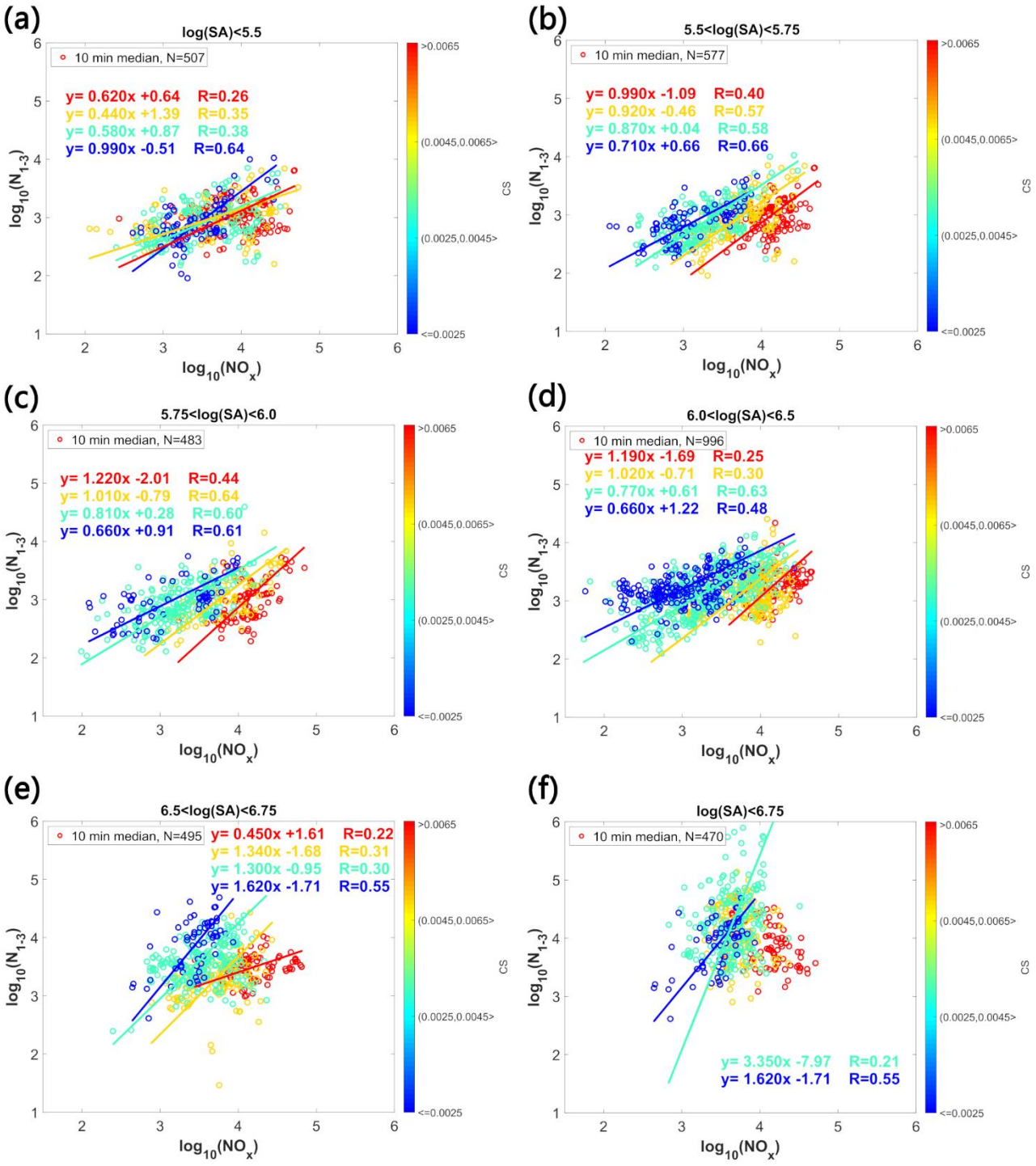

Figure S14. Correlation between the logarithm of NOx and the logarithm of sub-3 nm particles colored by the CS at the background station for data with the logarithm of SA in the range: (a) less than 5.50, (b) 5.50-5.75, (c) 5.75-6.00, (d) 6.00-6.50, (e) 6.50-6.75, and (f) more than 6.75. Lines represent bivariate fit done to data. The parameters of the fit are presented as an equation on the plot.

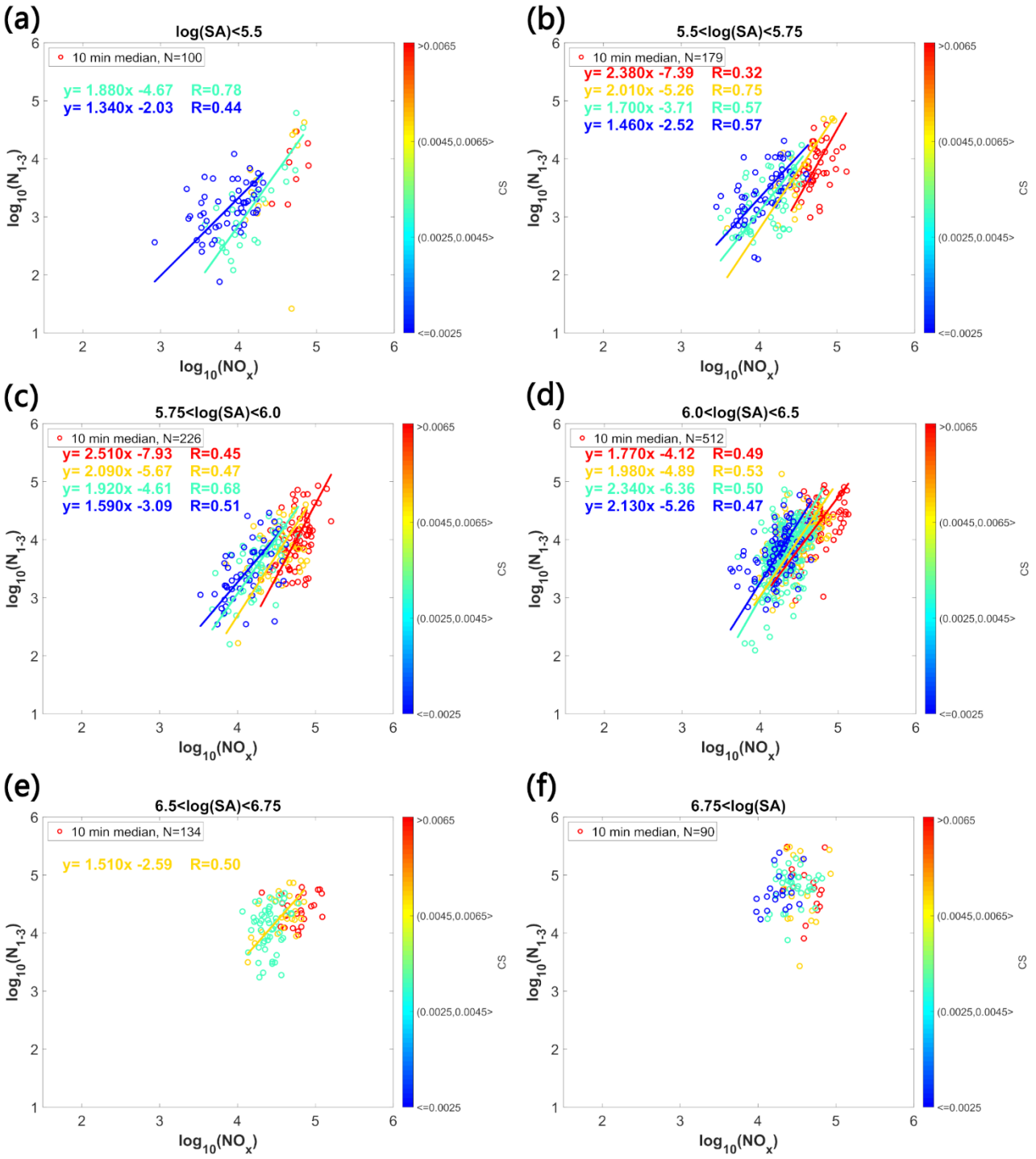

Figure S15. Correlation between the logarithm of NOx and the logarithm of sub-3 nm particles colored by the CS at the street canyon station for data with the logarithm of SA in the range: (a) less than 5.50, (b) 5.50-5.75, (c) 5.75-6.00, (d) 6.00-6.50, (e) 6.50-6.75, and (f) more than 6.75. Lines represent bivariate fit done to data. The parameters of the fit are presented as an equation on the plot.

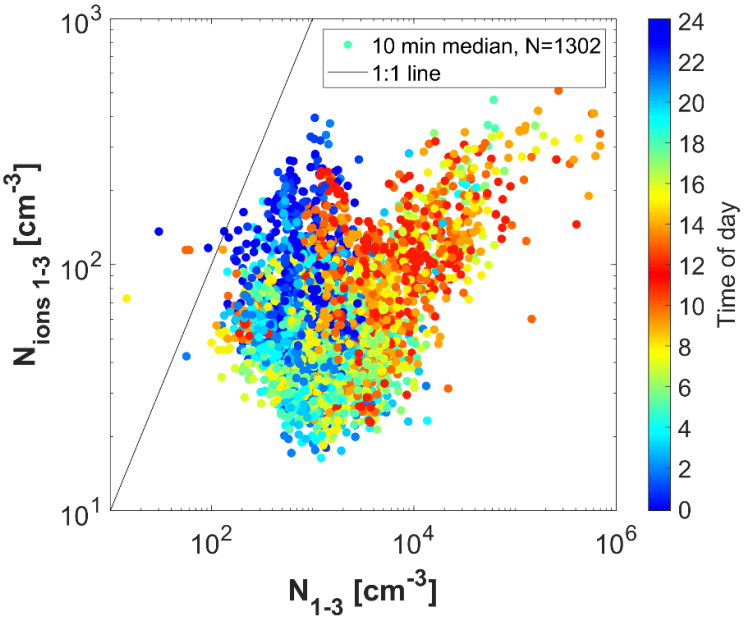

79 Figure S16. Correlation between the sub-3 nm particles concentration and concentration of ions with a diameter between
80 1 and 3 nm measured at the background station colored by the time of the day. The black line shows the 1:1 line.

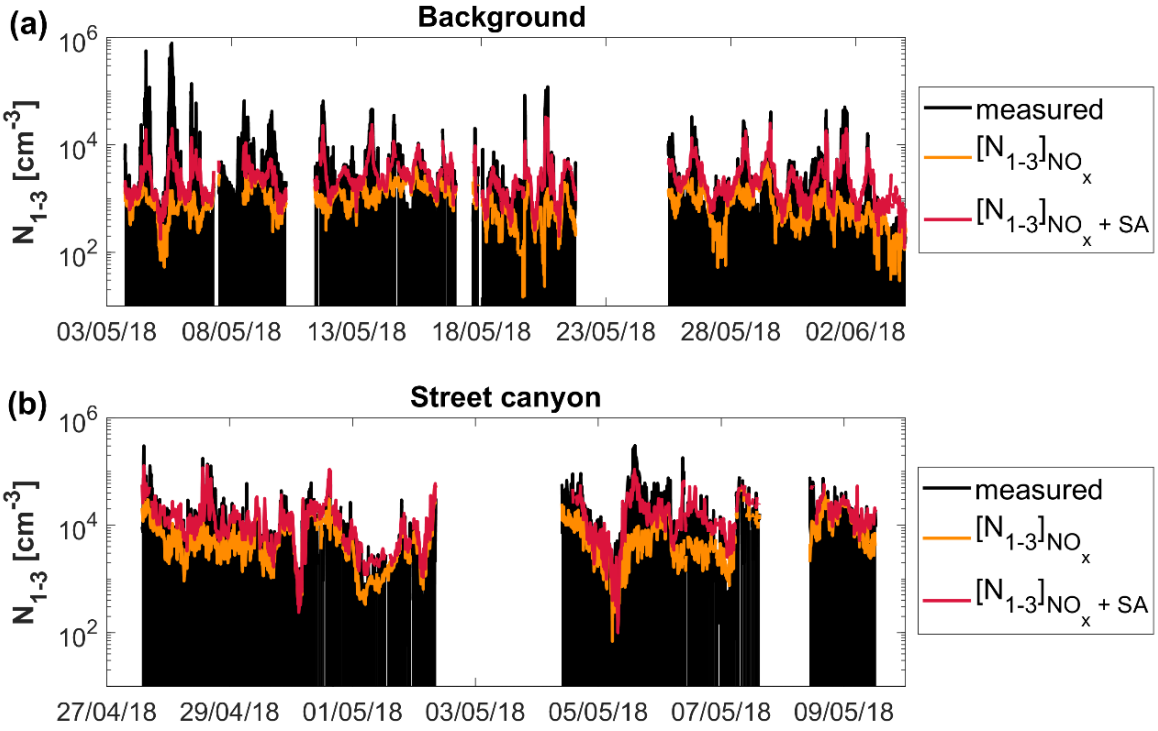

81 Figure S17. The time series (LT) of sub-3 nm particles concentration measured during the campaign (black) and estimated
82 based on NOx concentration (orange) and NO_x and SA concentrations (red) (a) at the background and (b) at the street
83 canyon station.

84

Table S2. The number of measured points (N), slope value, P-value, and Pearson correlation coefficient (R) of bivariate analysis result for common logarithms of N_{1-3}, SA, and NO_x concentrations.

Background station					Street canyon site				
Correlation between $\log_{10}(N_{1-3})$ and $\log_{10}(NO_x)$									
$\log_{10}$(SA) bin	N	Slope	P	R	$\log_{10}$(SA) bin	N	Slope	P	R
<= 5.50	507	0.64	<0.001	0.45	<= 5.50	100	1.40	<0.001	0.59
5.50-5.75	577	0.63	<0.001	0.48	5.50-5.75	179	1.29	<0.001	0.66
5.75-6.00	483	0.65	<0.001	0.48	5.75-6.00	226	1.44	<0.001	0.64
6.00-6.50	996	0.62	<0.001	0.41	6.00-6.50	512	1.73	<0.001	0.59
6.50-6.75	495	1.09	0.005	0.13	6.50-6.75	134	2.99	0.04	0.18
>6.75	470	1.07	0.002	-0.14	> 6.75	90	2.28	0.4	0.09
Correlation between $\log_{10}(N_{1-3})$ and $\log_{10}$(SA)									
$\log_{10}(NO_x)$ bin	N	Slope	P	R	$\log_{10}(NO_x)$ bin	N	Slope	P	R
<=3.00	521	0.89	<0.001	0.55	<=4.00	148	1.25	<0.001	0.39
3.00-3.50	940	0.94	<0.001	0.70	4.00-4.25	251	1.19	<0.001	0.54
3.50-3.75	687	0.94	<0.001	0.81	4.25-4.50	373	1.25	<0.001	0.59
3.75-4.00	637	0.92	<0.001	0.73	4.50-4.75	307	1.09	<0.001	0.51
4.00-4.25	469	0.96	<0.001	0.63	>4.75	162	1.32	<0.001	0.34
>4.25	274	0.65	<0.001	0.53	-	-	-	-	-

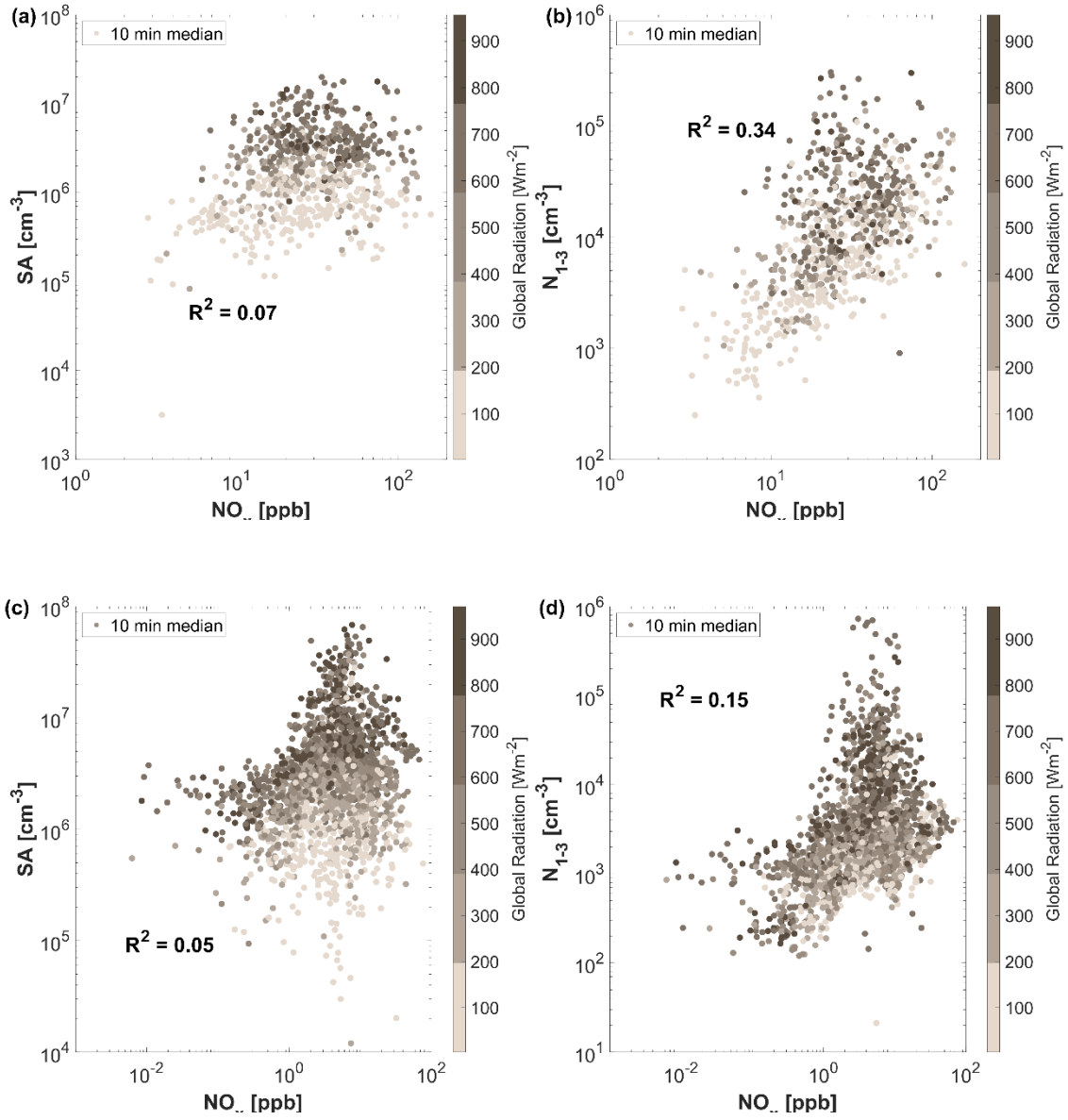

Figure S18. Relations between SA and NO_x concentrations (a,c) and sub-3 nm particles and NO_x concentrations (b,d) at the street canyon site (a,b) and the background station (c,d) calculated for the daytime (6-20) data with ten minutes resolution. The data points are colored with radiation level observed at the background station.

Table S3. Coefficient of determination (R^2) between SA and NO_x concentrations during daytime (10 minutes averaged data between 6 and 20 hours) at the study sites in different ranges of global radiation. The sample size is given in parenthesis and the correlations not significant at $p<0.05$ level are shown in italics.

	Low radiation (<20 W/m^2)	Medium radiation (20-300 W/m^2)	High radiation (>300 W/m^2)
Street canyon	0.018 (525)	0.067 (409)	*0 (371)*
Background	0.035 (21)	0.014 (740)	0.117 (1536)